

Particle Size Dependent Molecular Rearrangements During the Dehydration of Trehalose Dihydrate-*In Situ* FT-Raman Spectroscopy

Lynne S. Taylor,^{1,2} Adrian C. Williams,¹ and Peter York^{1,3}

Received March 19, 1998; accepted May 14, 1998

Purpose. (1) To characterise the different phases of trehalose using FT-Raman spectroscopy. (2) To monitor the changes in the structure of trehalose dihydrate on isothermal heating at 80°C.

Methods. Different phases of trehalose were prepared and FT-Raman spectra obtained. Trehalose dihydrate was sieved to <45µm and >425µm particle size fractions and FT-Raman spectra were obtained at various time intervals during heating at 80°C.

Results. During heating at this temperature, the spectra of a <45µm particle size fraction showed a loss of peak resolution with time and after 210 minutes resembled the spectrum of amorphous trehalose prepared by lyophilisation, indicating that the material was rendered amorphous by heating. In contrast, spectra obtained from a >425µm particle size fraction altered with time and became characteristic of the crystalline anhydrate. The approximate kinetics of this transformation to the anhydrate were monitored by analysis of peak intensity ratios with time. A two stage rearrangement was indicated; some functional groups appeared to manoeuvre into the spatial arrangement found in the anhydrate initially before the rest of the ring structure relaxed into this conformation. This may be due to some parts of the molecule being immediately affected by the loss of the water molecules on dehydration prior to the subsequent reorientation of the entire molecule into the anhydrate crystal lattice.

Conclusions. The <45µm particle size fraction becomes disordered on dehydration induced by heating at 80°C whilst the >425µm particle size fraction crystallises to the anhydrate under the same conditions.

KEY WORDS: FT-Raman spectroscopy; trehalose dihydrate; dehydration; crystalline; amorphous.

INTRODUCTION

The disaccharide α -trehalose is a naturally occurring non-reducing sugar whose presence in organisms which can withstand extremes of temperature has focused attention on this material as a stabilising agent for labile biological materials (1). Trehalose is a useful lyoprotectant for proteins and liposomes during freeze-drying operations (2). Although there is debate about the mechanisms by which carbohydrates preserve the structure and function of biological materials, both the hydrogen bonding ability (3) and the tendency of sugars to

form viscous amorphous states (4) are considered to be important factors. Since the amorphous phase is metastable relative to the crystalline material (5), phase transitions may occur during processing and on storage. Indeed, it has been proposed that the ability of trehalose to form a dihydrate on crystallisation from the amorphous state, thereby reducing the water content of the remaining amorphous phase, may contribute to the improved stabilising potential of this sugar in the dry state (6). The properties of crystalline forms of trehalose are therefore of interest.

Trehalose exists in two crystalline forms, specifically as a dihydrate and as an anhydrate and the crystal structure of both forms have been determined (7–9). On heating and subsequent dehydration, the dihydrate may either convert directly to the anhydrate or form an amorphous phase which may subsequently crystallise to the anhydrate (10); the route of anhydrate formation was found to depend on the particle size of the sample. This complex behaviour has been explained in terms of the kinetics of dehydration and the role that either water or lattice order may play in the solid-solid transformation.

Raman spectroscopy is a valuable technique for probing crystallinity and notably for examining the molecular nature of polymorphs and solvates (11–13). Amorphous and crystalline phases possess the same molecular species, hence spectral differences represent variations in molecular interactions within these different forms (12). Additionally FT-Raman spectroscopy enables *in situ* analysis of materials since no special sample preparation is necessary and, for most drug substances, high quality data can be collected over short time periods. For example, the dehydration of carbamazepine dihydrate was monitored with time using FT-Raman spectroscopy in conjunction with a heating accessory (14).

This study utilises FT-Raman spectroscopy to investigate molecular rearrangements during the dehydration of two particle size fractions of trehalose dihydrate at 80°C. Crystalline and amorphous forms of trehalose together with an aqueous solution were spectroscopically characterised in order to aid interpretation of phase changes during isothermal heating.

MATERIALS

α -Trehalose (α -D-glucopyranosyl α -D-glucopyranoside) was obtained as the dihydrate from Pfanstiehl Inc. (Waukegan, IL, USA). Trehalose anhydrate was prepared by heating the dihydrate at 120°C for 5 minutes, confirmed by a single endotherm with a peak at 212°C on analysis by differential scanning calorimetry (Perkin Elmer Series 7 DSC system at 10°C min⁻¹ in a vented pan (10)), consistent with published values for the melting point of the anhydrate (15). The X-ray diffraction powder pattern of this material, obtained between 5 and 40 degrees 2 θ (Siemens D5000 diffractometer (10)), was similar to the theoretical powder pattern generated from single crystal data (7) using Cerius software (MSI, Cambridge, UK). On recrystallisation from aqueous solution, trehalose dihydrate formed, confirmed by X-ray powder diffraction and thermogravimetric analysis (Perkin Elmer Series 7 Thermal Analysis System, heating rate 10°C min⁻¹, dry nitrogen purge) where the loss of 2 moles of water was observed. No evidence of decomposition was observed after such treatment. Amorphous trehalose was prepared by lyophilisation in a Dura-Stop Freeze-

¹ Drug Delivery Group, Postgraduate Studies in Pharmaceutical Technology, School of Pharmacy, University of Bradford, Bradford, West Yorkshire BD7 1DP, UK.

² Present address: School of Pharmacy, University of Wisconsin-Madison, 425 N. Charter St., Madison, Wisconsin 53706.

³ To whom correspondence should be addressed. (e-mail: p.york@bradford.ac.uk)

drier (FTS Systems, Stone Ridge, NY, USA) with primary drying at -35°C and secondary drying at a final temperature of 60°C . Material was confirmed as amorphous by X-ray powder diffraction analysis, with a water content of less than 0.5% as measured by Karl Fisher titrimetry (Model 701KF Titrimetric, Metrohm Ltd., Switzerland).

METHODS

Particle Size Fractionation

A nest of sieves (Endecott Ltd., London, UK) separated trehalose dihydrate (as supplied); apertures 425, 250, 150, 75 and $45\ \mu\text{m}$ were stacked, 200g powder sieved for 30 minutes (Endecott mechanical sieve shaker). Fractions $>425\ \mu\text{m}$ and $<45\ \mu\text{m}$ were utilised in this study.

FT-Raman Spectroscopy

FT-Raman spectra were obtained using a Bruker FRA-106 Raman module on an IFS 66 optics bench with a near-infrared Nd:YAG laser operating at 1064 nm. The maximum laser output was 1 W, with typically approximately 150 mW being used to excite the samples, and a liquid nitrogen-cooled germanium detector with an extended spectral band width that covered the range $3500\text{--}50\ \text{cm}^{-1}$ collected the backscattered radiation; Stokes scattering is reported. Band wavenumbers were calibrated against internal laser frequencies which provided vibrational band wavenumbers correct to $\pm 1\ \text{cm}^{-1}$.

Reference powder samples were lightly packed into an aluminium holder prior to analysis. 200 scans were obtained at room temperature within 5 minutes and co-added to give spectra with a signal to noise ratio >100 at a resolution of $4\ \text{cm}^{-1}$. An aqueous solution of trehalose (40% w/w) was analysed in a quartz cuvette with a mirrored rear surface, 200 scans again being collected at $4\ \text{cm}^{-1}$ resolution.

Elevated temperature studies used a novel environmental chamber adapted from a Graseby-Specac 19930 variable-temperature diffuse reflectance accessory with the window removed (16). Sample temperature, monitored by a thermocouple, was increased to 80°C at $10^{\circ}\text{C}\ \text{min}^{-1}$ using a programmable temperature controller P/N 20120 series (Specac Ltd., UK). The sample was held at 80°C and spectra (200 scans) were obtained at 20 minute intervals over 210 minutes. Spectra show no evidence of thermal artefacts due to sample heating by the laser.

RESULTS

Spectroscopic Characterization of the Dihydrate and Anhydrous Forms

The FT-Raman spectrum of trehalose dihydrate in Figure 1 is compared with that of the anhydrate, the amorphous form and aqueous solution. The structure of trehalose is shown in Figure 2. The spectra of the two particle size fractions of the dihydrate were identical indicating that the fractionation process had not led to any detectable structural alterations. However, subtle differences are present between the dihydrate and the anhydrous material.

The spectral region between 3015 and $2880\ \text{cm}^{-1}$ (Figure 1) is composed of vibrations arising from the asymmetrical and

symmetrical stretching of the ring CH modes. Abbate and co-workers (17) have assigned these CH stretching vibrations in the dihydrate spectrum as follows: 2994 and $2974\ \text{cm}^{-1}$ (C-6-H), $2951\ \text{cm}^{-1}$ (C-2-H), shoulder at $2945\ \text{cm}^{-1}$ (C-1-H), $2915\ \text{cm}^{-1}$ (C-3-H), shoulder at $2908\ \text{cm}^{-1}$ (C-4-H), and 2899 (C-5-H). In the anhydrate several differences are present in this spectral region as can be seen from Figure 1. In the dihydrate spectrum the C-1-H vibration occurs as a shoulder at $2945\ \text{cm}^{-1}$ on the C-2-H peak. The new peak seen in the anhydrate spectrum at $2934\ \text{cm}^{-1}$ is assigned to this C-1-H vibration which has shifted position in conjunction with the C-2-H stretching vibration which shifts from $2951\ \text{cm}^{-1}$ in the dihydrate spectrum to $2949\ \text{cm}^{-1}$ in the anhydrate. The change in the position of the C-1-H vibration would reflect a change in the conformation of the glycosidic linkage at C1. In addition, in the anhydrate spectrum there is an enhancement in the intensity of the C-6-H peak seen at $2973\ \text{cm}^{-1}$ and the vibration at $2994\ \text{cm}^{-1}$ is replaced by one at $3013\ \text{cm}^{-1}$. Thus the major differences between the dihydrate and anhydrate are reflected by the positions of the C-1-H and C-6-H vibrations.

The lower regions of the spectrum, below $1500\ \text{cm}^{-1}$, contain the O-C-H, C-C-H, and C-O-H deformations and the C-C and C-O stretching modes. For carbohydrates, most of the vibrations in this region of the spectrum arise from coupled modes rather than characteristic group frequencies. Thus the majority of peaks contain contributions from more than one functional group making group frequency assignments difficult (18). Characteristic regions of the spectra can however be defined (19). Spectra of carbohydrates composed of glucose tend to be quite similar in the region below $1500\ \text{cm}^{-1}$ as most of the vibrations arise from the isolated glucose unit with only a small contribution arising from inter-residue coupling (20). Extensive analysis has been carried out on glucose describing the normal modes of vibration and this data can also be used to aid spectral interpretation (18).

The pattern of vibrations between 950 and $700\ \text{cm}^{-1}$, shown in Figure 1, is characteristic of the conformation at the anomeric carbon (20). Based on infrared spectroscopic studies of several D-glucopyranose derivatives, bands sensitive to the anomeric conformation have been assigned and classified as type 1, 2 and 3 bands (21). Type 2 bands, typically seen at $844 \pm 8\ \text{cm}^{-1}$, arise from the anomeric C-H deformation and only this band can be used to differentiate the anomeric glycosidic linkage (22). In trehalose the conformation is α -at both of the anomeric carbons and this is reflected by the presence of a type 2 band at $839\ \text{cm}^{-1}$. A type 1 band occurs at $912\ \text{cm}^{-1}$. Based both on the normal coordinate analysis of glucose and deuteration studies, this peak contains contributions from C-1-H, CH_2 and C-O-H bending motions (20). The type 3 band around $766\ \text{cm}^{-1}$ in the infrared spectrum of sugars is absent in the Raman spectrum of trehalose, as is the case for glucose (23). The anomeric region of the spectrum of the anhydrate displays some differences in both the relative intensities and positions of these vibrations when compared with that of the dihydrate. The relative intensities of the peaks forming the doublet at around $930\text{--}900\ \text{cm}^{-1}$ are altered with the higher wavenumber peak increasing in prominence in the anhydrate and the lower wavenumber vibration shifts from 912 to $904\ \text{cm}^{-1}$. The peak at $957\ \text{cm}^{-1}$ in the dihydrate is absent in the anhydrate spectrum. On changing from the dihydrate to the anhydrate, the type 2 band shifts to lower wavenumber whilst the shoulder on this

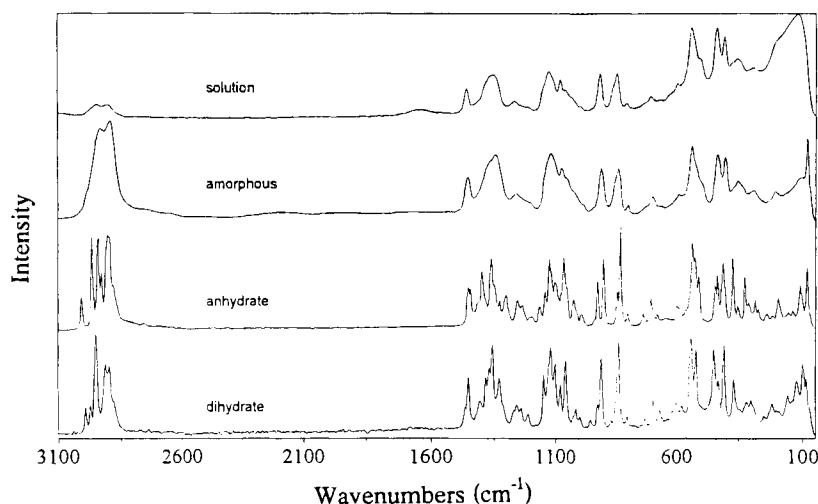


Fig. 1. FT-Raman spectra of various phases of trehalose. The solution contained 40% w/w trehalose and the amorphous trehalose had a water content of less than 0.5%.

band develops into a peak at 848 cm^{-1} . These changes indicate that although there is no difference in the anomeric configuration in the dihydrate and the anhydrate, there is some variation in the conformation around the glycosidic linkage in the two forms.

The "skeletal" wavenumber region is between 700 and 200 cm^{-1} (19), for which assignment of glucose bands has been reported (18). Here, trehalose spectral features are likely to arise from similar vibrational modes as in glucose. Thus this region contains C-C and C-C-C skeletal modes with CO and CCO bending vibrations and subtle differences are present between the dihydrate and anhydrate. For example, the doublet at around 540 cm^{-1} in the dihydrate spectrum forms a broad peak with two sharp shoulders in the anhydrate spectrum (see Figure 1). There are also differences in the relative intensities of the peaks around 450 cm^{-1} and 430 cm^{-1} .

The $150\text{-}50\text{ cm}^{-1}$ region of the Raman spectrum contains bands arising from lattice vibrations corresponding to librations and translations of the entire molecule in the lattice, characteristic of crystal structure and sensitive to local order or disorder. Incorporation of the solvent molecules into the crystal lattice will produce a unit cell different to that of the anhydrate (24) and differences in this region of the spectrum would thus be anticipated. The spectra differ with peaks at 99 and 123 cm^{-1}

in the dihydrate spectrum compared to at 112 cm^{-1} in the anhydrate spectrum. It should be noted that the line at around 84 cm^{-1} is the filter line.

Spectroscopic Characterization of Amorphous Trehalose

The spectrum of amorphous trehalose in Figure 1 can be compared with the spectra of the two crystalline forms and a 40% w/w trehalose solution. Relative to the crystalline forms, the spectrum of amorphous trehalose has broader, less well resolved peaks, and is very similar to that obtained from a solution. Since the amorphous state can be regarded as a non-equilibrium supercooled liquid (5) this similarity is not unexpected and reflects the random nature of both systems. Some variation in hydrogen bonding between trehalose molecules in the condensed state compared to hydrogen bonding in aqueous solution might be expected and there is some evidence of such differences in the two spectra.

The conformation of the glycosidic linkage of trehalose in solution is reported to be similar to that in both the dihydrate and the anhydrate forms, and the linkage conformation is relatively inflexible (25). Here, the conformation of the glycosidic linkage in amorphous trehalose is similar to that in solution as reflected by the similarity of the position and shape of the type 1 and 2 bands at 913 and 842 cm^{-1} respectively as shown in Figure 1. These broad bands also occur over approximately the same wavenumber region as the type 1 and 2 bands in the dihydrate and anhydrate spectra suggesting that the conformation in both solution and amorphous phases is similar to that found in the crystalline phases. Additionally, the loss of lattice vibration region of the spectrum below 150 cm^{-1} reflect the disorder in the solution and the amorphous phases and similar changes have been observed for other systems (12).

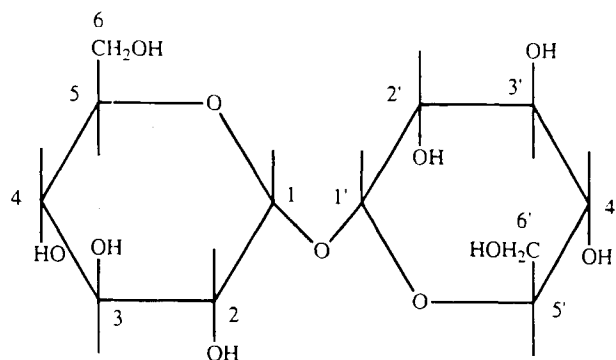


Fig. 2. Structure of trehalose showing numbering of carbons.

Isothermal Heating of the Less than $45\text{ }\mu\text{m}$ Particle Size Fraction

Figure 3 shows spectra obtained over time for the $<45\text{ }\mu\text{m}$ particle size fraction of trehalose dihydrate at 80°C . On heating, all the peaks rapidly lose definition, becoming less

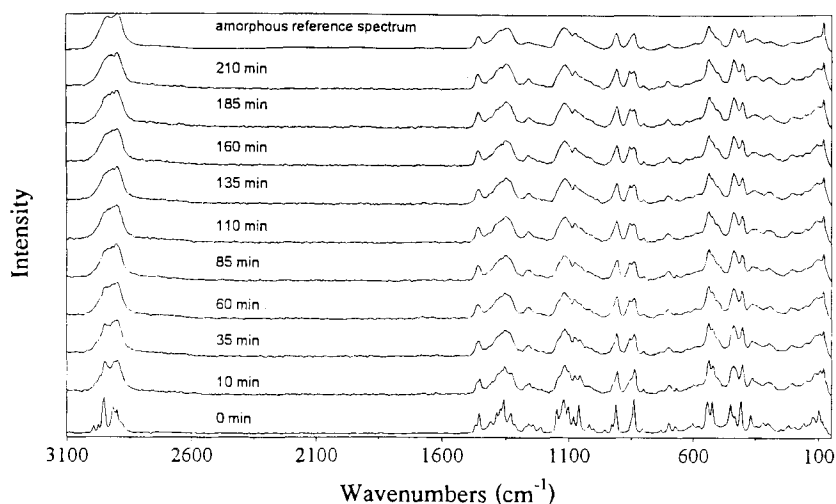


Fig. 3. FT-Raman spectra obtained at various time intervals during the heating of a $<45 \mu\text{m}$ particle size fraction of trehalose dihydrate at 80°C .

well resolved with considerable broadening. Such vibrational broadening is characteristic of a disordered amorphous state. The loss of structure is especially noticeable if the wavenumber region below 150 cm^{-1} , where the peaks arise from crystal lattice librations, is studied; the lattice modes of the material after 210 minutes at 80°C are very similar to those of amorphous trehalose. However the loss of peak resolution in the spectrum of the dehydrated material is not quite as extensive as in the spectrum of amorphous trehalose. This can be noted, for example, from the profile of the CH stretching peaks around $3100\text{--}2800 \text{ cm}^{-1}$. Additionally, the sharp peak at 834 cm^{-1} in the dihydrate spectrum is replaced by a doublet (861 cm^{-1} and 843 cm^{-1}), not seen in the amorphous spectrum where only a single peak is present. The fact that the two spectra are not identical suggests that the dehydrated phase is not as disordered as the lyophilised material.

Isothermal Heating of the Greater than $425 \mu\text{m}$ Particle Size Fraction

Spectra of the $>425 \mu\text{m}$ particle size fraction of heated dihydrate with time are in Figure 4. The consequences of heating at 80°C for this powder size, summarised in Table 1, are very different when the spectra are compared with those obtained for the $<45 \mu\text{m}$ fraction. A comparison of the spectrum obtained after 210 minutes at 80°C with that of the anhydrate reveals that they are nearly identical indicating that heating has converted the dihydrate into the anhydrous form. Minor differences in the two spectra may arise from a small percentage of unconverted dihydrate.

Figure 4 shows the changes occurring in the CH stretching region with time. Notably, the ratio of the peak intensities at 2915 (C-3-H) and 2899 (C-5-H) cm^{-1} gradually alters with time with the lower wavenumber peak becoming of greater intensity, reversing the pattern seen in the spectrum of the dihydrate prior to heating. Concomitant with the appearance of a vibration at 3013 cm^{-1} , the peak at 2994 cm^{-1} decreases and that at 2974 cm^{-1} increases in intensity after a short period of heating. All of these peaks are associated with the C-6-H vibration. After 35 minutes a weak peak appears at 2934 cm^{-1} (C-1-H) which increases in intensity with time.

Examination of the spectra below 2000 cm^{-1} reveals numerous gradual changes in the pattern of peaks as the material is held at 80°C . Changes occurring in the anomeric region between 950 and 700 cm^{-1} are of interest as these monitor the conformation of the glycosidic linkage (see Figure 4). The weak peak at 928 cm^{-1} increases considerably in intensity up to 35 minutes at 80°C whilst the adjacent peak at 912 cm^{-1} gradually broadens then narrows with a shift to a lower wavenumber. The peak at 839 cm^{-1} initially has a slight shoulder which increases in prominence with time on heating.

Examination of the skeletal and CCO and CO modes at approximately $600\text{--}400 \text{ cm}^{-1}$ in Figure 4 also reveals gradual changes in peak properties with time, (see Table 1). Changes in the spectral region between 150 and 50 cm^{-1} also occur progressively with time (see Figure 6).

Data in Figure 4 demonstrate that some of the spectral changes occur and are completed over a more rapid time scale than others. In order to investigate this phenomenon in more detail, the time course of the conversion of the dihydrate to the anhydrate was followed by monitoring the relative intensities of 4 pairs of peaks, that is I_{2994}/I_{3013} , I_{904}/I_{928} , I_{542}/I_{430} and I_{450}/I_{430} . Although the peak positions altered slightly in some cases, following the relative intensities provides an approximate indication of the kinetics of the conversion. From the results in Figures 5 and 6, it is apparent that the rate of conversion is sensitive to the functional group monitored. The CH_2 stretching modes (I_{2994}/I_{3013}) and the vibrations arising from the type 1 anomeric bands (I_{904}/I_{928}) alter abruptly between 0 and 35 minutes with little change observable after this time period (Figure 5). In contrast the vibrations arising as a result of the skeletal CC, CCO and CO stretching and bending deformations (I_{542}/I_{430} and I_{450}/I_{430}) alter towards the anhydrous form in a more gradual manner as shown in Figure 6. It thus appears that on rearrangement from the dihydrate to the anhydrate on dehydration, certain functional groups relax into the new conformation characteristic of the anhydrate faster than others.

DISCUSSION

The minor of spectral differences observed between trehalose dihydrate and anhydrate are expected for systems where

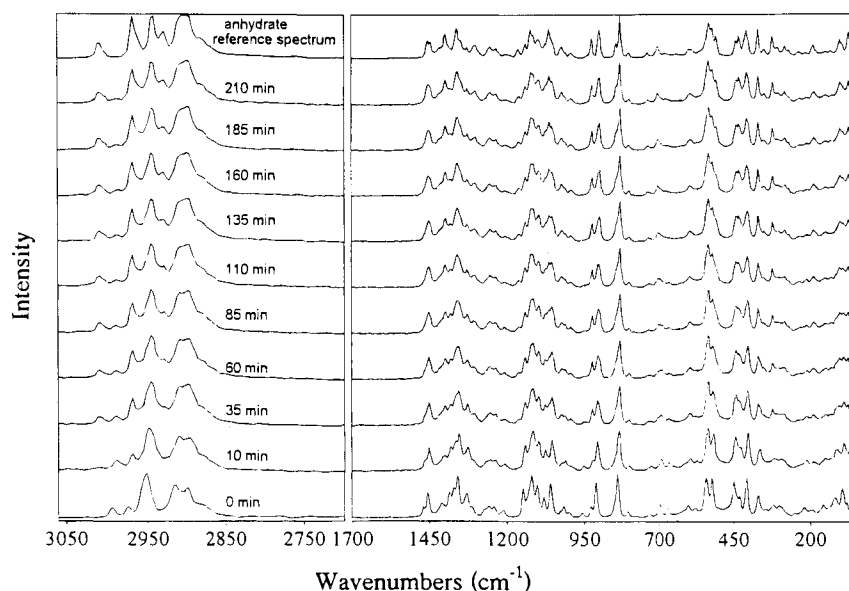


Fig. 4. FT-Raman spectra obtained at various time intervals during the heating of a $>425 \mu\text{m}$ particle size fraction of trehalose dihydrate at 80°C .

the molecular species is identical but the functional groups are exposed to slightly different environments as a result of differences in crystal structure. Removal of the water molecules from the dihydrate with rearrangement into a new anhydrous

crystalline form with a different unit cell will obviously affect both the hydrogen bonding pattern and the orientation of groups relative to one another within the crystal lattice. Thus the vibrational frequency of associated groups and the region of the

Table 1. Summary of FT-Raman Spectral Changes Occurring on Conversion of $>425 \mu\text{m}$ Trehalose Dihydrate to Anhydrate on Heating^a

Dihydrate		Anhydrate	
Wavenumber (cm ⁻¹)	Comments-behavior on heating	Wavenumber (cm ⁻¹)	Comments
CH Stretching Region			
2994w	Intensity decreases.	3013w	Appears on heating dihydrate after 35 min.
2974w	Intensity increases, shifts to 2972cm ⁻¹ .	2972s	
2951s	Shoulder lost, peak shifts down.	2948s	Appears on heating dihydrate.
2915s	Decrease in intensity relative to peak at 2899cm ⁻¹ .	2934m	
2899m	Increase in intensity relative to peak at 2915cm ⁻¹ .	2908s	
		2906s	
		2887sh	
Anomeric Region			
957w	Decrease in intensity.	930m	Develops from shoulder on 839cm ⁻¹ peak in dihydrate.
928m	Increase in intensity relative to 912cm ⁻¹ .	904s	
912s	Shift to 904cm ⁻¹ .	848m	
839s	Shoulder on peak increases in intensity, shift to 834cm ⁻¹ .	834s	
600-400cm ⁻¹ Skeletal modes-CC, CCC with δCCO and δOCO			
542s	Shifts to 536cm ⁻¹ .	536s	Appears on heating dihydrate.
522s	Decrease in intensity relative to 542cm ⁻¹ , shift to 526cm ⁻¹ .	526m	
450s	Decrease in intensity relative to 431cm ⁻¹ , shift to 447cm ⁻¹ .	513m	
431m	Increase in intensity relative to 450cm ⁻¹ , shift to 436cm ⁻¹ .	447m	
408s	Shift to 413cm ⁻¹ .	436m	
		413s	

^a w = weak, m = moderate, s = strong, sh = shoulder.

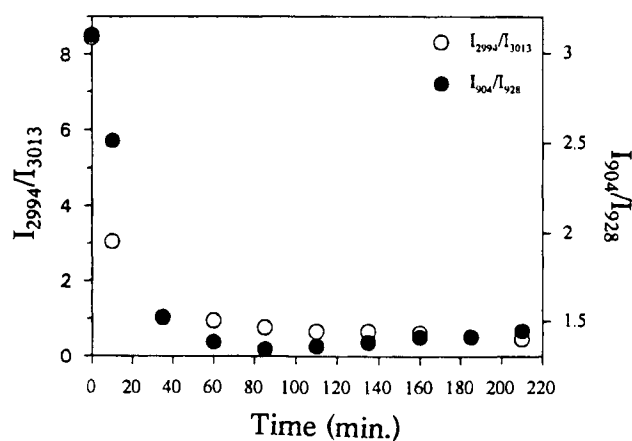


Fig. 5. Changes in peak intensity ratios with time at 80°C for the CH stretching modes and type 1 anomeric bands of trehalose dihydrate (>425 μm).

spectrum associated with the lattice vibrations themselves are affected.

The positions and interactions of the two water molecules within the dihydrate crystal lattice should be considered in order to understand the consequences of their removal. From single crystal data, one of the water molecules (W1) has four hydrogen bonds in a distorted tetrahedral configuration, whilst the other water molecule, W2, has three hydrogen bonds in an approximately pyramidal arrangement. Each glucopyranosyl moiety is linked to the other within the same molecule indirectly through the two different water molecules, in contrast to other sugars such as sucrose where there is direct intramolecular hydrogen bonding (7). Thus within the same trehalose molecule, the water molecule W1 acts as a bridge between O(2) and O(4') and W2 forms a bridge between O(2) and O(6'). Water molecules also intermolecularly hydrogen bond; bonds between W1 and the OH(2') groups of two trehalose molecules results in the formation of an infinite spiral chain of molecules in the *c* crystallographic direction. Another intermolecular hydrogen bond between W2 and O(3) links the molecules in the *b* direction.

It has been suggested that the indirect intramolecular hydrogen bonds, mediated through water, may influence the

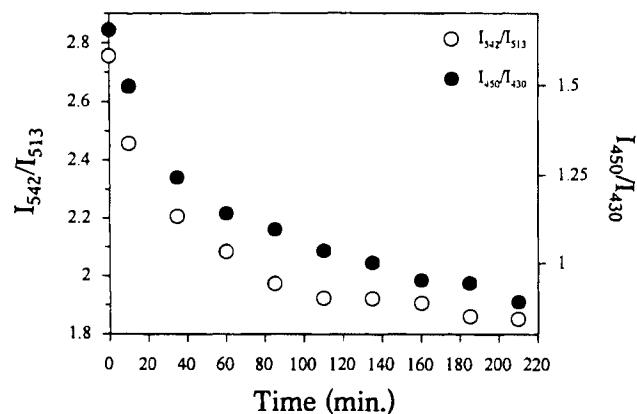


Fig. 6. Changes in peak intensity ratios with time at 80°C for groups associated with skeletal modes and CCO, OCO deformations of trehalose dihydrate (>425 μm).

torsion angle about the I-1' glycosidic linkage (8). Dehydration would thus be expected to influence the torsion angles around the glycosidic linkage and it is known that the two glycosidic-linkage torsion angles are more similar in the anhydrate: +60.8° and +60.1° versus +74.8° and +61.7° in the dihydrate. The D-glucopyranosyl groups are therefore closer to having the ideal-chair conformation and are more symmetrically orientated about the central, glycosidic oxygen atom in the anhydrate compared to the dihydrate. These differences in the conformation of the glycosidic linkage in the dihydrate and anhydrate explain the observed differences in the pattern of vibrations in the anomeric region.

The removal of the intramolecular bridges on dehydration and the subsequent change in conformation would also be expected to alter the environment of the hydrogen atoms, hence the variation in the CH stretching vibrations between the anhydrate and dihydrate. The C1-H and C6-H vibrations show the biggest variations between the two forms. The difference in the C1-H vibration can be accounted for by the change in conformation around the glycosidic linkage whilst those in C6-H vibrations are likely to arise as a consequence of the involvement of the C6 hydroxyl group in hydrogen bonding with water. Since C6 is not involved in the ring structure, the changed environment on removal of the water molecule may be greater than for ring carbons.

Since all of the sugar hydroxyl groups are involved in hydrogen bonding in both the anhydrate and dihydrate (7,9), hydrogen bonds lost with the removal of water will necessitate the formation of new hydrogen bonds in the anhydrate between the hydroxyl groups. Additionally, in the dihydrate, the ring oxygen does not accept hydrogen bonds whilst in the anhydrate, the ring oxygens are included in the hydrogen bonding scheme through bifurcated bonds. These changes in the hydrogen bonding patterns are likely to account for the observed variations in the C-O stretching and bending regions of the spectrum.

The particle size dependence of the dehydration behaviour of trehalose dihydrate on isothermal heating, followed using FT-Raman spectroscopy, is in good agreement with previous studies using different experimental techniques (10). In addition, the short sampling time required for acquisition of the spectroscopic data enables the molecular rearrangements during dehydration to be monitored. Possible explanations for the particle size dependence of the phase transformations of trehalose dihydrate on dehydration have been extensively discussed previously (10). A consequence of water removal from the small particle size fraction is collapse of the crystal structure to form a more disordered phase. However dehydration of the dihydrate at 80°C does not appear to result in the same level of disorder as in amorphous trehalose prepared by lyophilisation from aqueous solution. Whilst it is apparent, from a consideration of role of the water molecules in the crystal structure, that dehydration must result in a collapse of crystal structure, the mobility of the new phase must be also be taken into account. Dry amorphous trehalose is known to have a glass transition temperature of around 119°C (26). Since the viscosity of amorphous material at temperatures below the glass transition temperature is known to be very high (5), the mobility of any disordered phase formed by dehydration at 80°C (and presumably not containing any moisture since dehydration is occurring) will be limited. Indeed, the formation of a completely disordered system by dehydration of a crystal hydrate may not be possible at temperatures below

the glass transition of the amorphous phase of that material. The ordered arrangement of the molecules in the lattice prior to dehydration would presumably have some impact on the arrangement of the molecules subsequent to dehydration leading to some residual order, the degree of which might be related to the temperature of dehydration relative to the glass transition temperature. It is interesting to note that a new partially crystalline form of trehalose has been reported (27), formed by dehydration under vacuum at 50°C but with a Raman spectrum essentially identical to that obtained by dehydrating the <45 μm particle size fraction at 80°C in this study. Clearly this is not a new crystalline form of anhydrous trehalose but the disordered product of the dehydrated dihydrate.

The approximate kinetics of dehydration and the consequent molecular rearrangement to the anhydrate could be followed for the >425 μm particle size fraction of trehalose dihydrate by monitoring the ratios of various peaks assigned to different functional groups. It is interesting to note that some vibrations resemble those seen in the anhydrate after only a short time period at 80°C whilst others change towards the anhydrate in a more gradual manner. One explanation for this observation could be that the environment of some groups is immediately affected by the loss of the water molecule; this necessitates an immediate relaxation into the anhydrous conformation. After the loss of the water, the molecules as a whole must rearrange into a new crystal lattice and this occurs more gradually with time. Thus it is expected that the peaks characteristic of the lattice vibrations (150–50 cm^{-1}) and those arising from the ring structure would show a gradual change reflecting these molecular rearrangements and this is indeed the case. In contrast, a group more directly associated with the water molecules would show a rapid change, as is seen for the C6-H (2994–3013 cm^{-1}) vibration where the hydroxyl attached to the C6 is involved in an indirect intramolecular hydrogen bond mediated through a water molecule.

Changes in the physical form of trehalose in a pharmaceutical formulation would have an impact on drug stability dependent on the particular excipient role played by trehalose. Byrn et al. (28) and York (29) describe in detail the need for control of the physical form of both active ingredients and excipients. For example, when included in a formulation to stabilise biological molecules, trehalose must be present in the same phase as the active material, and this will be the amorphous state. Any crystallisation during processing or storage would result in phase separation with crystallisation to a hydrate form considered more beneficial for product stability than to an anhydrate state (6). In other instances, the more hygroscopic amorphous phase, with increased mobility relative to the crystalline forms, might enhance drug instability. Clearly knowledge of the physical stability of the different phases of trehalose is important when producing and attempting to maintain the desired form in a pharmaceutical formulation.

SUMMARY

FT-Raman spectroscopy has been used to characterise the different phases of trehalose namely the two crystalline forms, dihydrate and anhydrate, the amorphous phase and in aqueous solution. Subtle differences are present between the two crystalline forms, whilst the amorphous material has a spectrum similar

to an aqueous solution with minor differences being ascribed to variations in the hydrogen bonding pattern.

The dehydration behaviour of trehalose dihydrate at 80°C was interpreted with the aid of the spectral data gathered for the different forms and was found to depend on the particle size. Heating at 80°C altered the spectral features of the >425 μm particle size fractions which, with time, became characteristic of the anhydrate. These spectral data are consistent with previous studies using different techniques which also showed a conversion from the dihydrate to the anhydrate on heating and dehydration (10). The spectroscopic evidence supports a direct conversion to the anhydrate, providing structural information on a molecular level. The changes observed occur progressively with time which indicates that the dihydrate does not pass through a monohydrate intermediate. Some functional groups apparently manoeuvre into the spatial arrangement found in the anhydrous form prior to the ring structure relaxing into this conformation. It is suggested that the groups which show a rapid initial spectral changes are those which are immediately affected by the loss of the water molecules whilst the gradual changes represent the rearrangement of the molecules as a whole into the anhydrate crystal lattice. The changes in the spectrum of the small particle size fraction on heating indicate that a disordered structure is formed and are also consistent with previous studies. It is suggested that the extent of disorder induced by dehydration of a crystalline hydrate may depend on the temperature of dehydration relative to the glass transition temperature of the completely amorphous material.

ACKNOWLEDGMENTS

The authors gratefully acknowledge EPSRC and SmithKline Beecham for the provision of a CASE award for LST.

REFERENCES

1. B. Roser. Trehalose Drying—A Novel Replacement For Freeze-Drying. *Biopharm.* **4**:47–52. (1991).
2. L. M. Crowe, D. S. Reid, and J. H. Crowe. Is Trehalose Special For Preserving Dry Biomaterials? *Biophys. J.* **71**:2087–2093 (1996).
3. J. F. Carpenter and J. H. Crowe. An Infrared Spectroscopic Study Of The Interactions Of Carbohydrates With Dried Proteins. *Biochem.* **28**:3916–3922 (1992).
4. H. Levine and L. Slade. Another View Of Trehalose For Drying And Stabilizing Biological Membranes. *Biopharm.* **5**:36–40 (1992).
5. B. C. Hancock and G. Zografi. Characteristics And Significance Of The Amorphous State. *J. Pharm. Sci.* **86**:1–12 (1997).
6. B. J. Aldous, A. D. Auffret, and F. Franks. The Crystallisation Of Hydrates From Amorphous Carbohydrates. *Cryo-Letters* **16**:181–186 (1995).
7. G. M. Brown, D. Rohrer, B. Berking, C. A. Beevers, R. O. Gould, and R. Simpson. The Crystal Structure Of α,α -Trehalose Dihydrate From Three Independent X-Ray Determinations. *Acta Cryst.* **B28**:3145–3158 (1972).
8. T. Taga, M. Senna, and K. Osaki. The Crystal And Molecular Structure Of Trehalose Dihydrate. *Acta Cryst.* **B28**:3258–3263 (1972).
9. G. A. Jeffrey and R. Nanni. The Crystal Structure Of Anhydrous α,α -Trehalose At - 150°. *Carbohydr. Res.* **137**:21–30 (1985).
10. L. S. Taylor and P. York. Characterisation Of The Phase Transitions Of Trehalose Dihydrate On Heating And Subsequent Dehydration. *J. Pharm. Sci.* (1998) In Press.
11. H. G. Brittain. Spectral Methods For The Characterization Of Polymorphs and Solvates. *J. Pharm. Sci.* **86**:405–412 (1997).

12. P. N. Prasad, J. Swiatkiewicz, and G. Eisenhardt. Laser Raman Investigation Of Solid State Reactions. *Appl. Spectrosc. Rev.* **18**:59–103 (1982).
13. D. E. Bugay and A. C. Williams. Vibrational Spectroscopy. In H. G. Brittain (ed.), *Physical Characterization of Pharmaceutical Solids*, Marcel Dekker Inc., New York, 1995, pp 59–91.
14. L. E. McMahon, P. Timmins, A. C. Williams, and P. York. Characterisation Of Dihydrates Prepared From Carbamazepine Polymorphs. *J. Pharm. Sci.* **86**:1064–1069 (1996).
15. F. Shafizadeh and R. A. Susott. Crystalline Transitions Of Carbohydrates. *J. Org. Chem.* **28**:3710–3715 (1973).
16. H. G. M. Edwards, D. W. Farwell, J. M. C. Turner, and A. C. Williams. Novel Environmental Control Chamber For FT-Raman Spectroscopy: Study Of In Situ Phase Change Of Sulphur. *Appl. Spectrosc.* **51**:101–107 (1997).
17. S. Abbate, G. Conti, and A. Naggi. Characterisation Of The Glycosidic Linkage By Infrared And Raman Spectroscopy In The C-H Stretching Region: α,α -trehalose and α,α -trehalose-2,3,4,6,6-*d*₁₀. *Carbohydr. Res.* **210**:1–12 (1991).
18. P. D. Vasko, J. Blackwell, and J. L. Koenig. Infrared And Raman Spectroscopy Of Carbohydrates. Part II. Normal Coordinate Analysis of α -D-Glucose. *Carbohydr. Res.* **23**:407–416 (1972).
19. M. Matlouthi and J. L. Koenig. Vibrational Spectra Of Carbohydrates. *Adv. Carb. Chem. Biochem.* **44**:7–89 (1986).
20. J. J. Cael, J. L. Koenig, and J. Blackwell. Infrared And Raman Spectroscopy Of Carbohydrates. Part IV. Identification Of Configuration- And Conformation-Sensitive Modes For D-Glucose By Normal Coordinate Analysis. *Carbohydr. Res.* **32**:79–91 (1974).
21. S. A. Barker, E. J. Bourne, R. Stephens, and D. H. Whiffen. Infrared Spectra Of Carbohydrates. Part II. Anomeric Configuration of Some Hexo- And Pento-pyranoses. *J. Chem. Soc.* **171**:3468–3473 (1954).
22. A. T. Tu. *Raman Spectroscopy In Biology. Principles And Applications*. John Wiley and Sons, Inc, New York, 1982.
23. L. S. Taylor, P. York, A. C. Williams, and V. Mehta. Characterisation of Frozen Glucose Solutions. *Pharma. Dev. Tech.* **2**:395–402 (1997).
24. R. K. Khankari and D. J. W. Grant. Pharmaceutical Hydrates. *Thermochim. Acta.* **248**:61–79 (1995).
25. C. A. Duda and E. S. Stevens. Trehalose Conformation In Aqueous Solution From Optical Rotation. *J. Am. Chem. Soc.* **112**:7406–7407 (1990).
26. L. S. Taylor. Carbohydrates As Protein Stabilising Agents. PhD Thesis, University of Bradford, Bradford, UK 1996.
27. A. M. Gil, P. S. Belton, and V. Felix. Spectroscopic Studies Of Solid α,α Trehalose. *Spectrochim. Acta.* **52**:1649–1659 (1996).
28. S. Byrn, R. Pfeiffer, M. Ganey, C. Hoiberg, and G. Poochikian. Pharmaceutical Solids: A Strategic Approach To Regulatory Considerations. *Pharm. Res.* **12**:945–954, (1995).
29. P. York. Solid-State Properties Of Powders In The Formulation And Processing Of Solid Dosage Forms. *Int. J. Pharm.* **14**:1–28 (1983).